THE CRACKING OF SOL-GEL FILMS DURING DRYING

TERRY J. GARINO
Sandia National Laboratories, Electronic Ceramics Division 1842, Albuquerque, NM 87185

SAND--89-2804C

DE90 010821

ABSTRACT

The cracking behavior of acidic silica sol-gel films during drying and low temperature heat treatment was studied. Films that cracked during drying exhibited a variety of unusual crack morphologies including sinusoidal cracks and parallel crack pairs. The effects of the water content of the sol and temperature on the critical thickness above which cracking of the films occurred were determined. The critical thickness decreased with increasing water content because the surface tension of the liquid in the pores of the gel increases with water content and because sols with low water concentrations did not gel until the solvent had evaporated. To determine why the critical thickness decreased with temperature, thermal analysis and shrinkage measurements of both constrained and unconstrained films were performed. Thermogravimetric analysis indicated that rapid weight loss occurred in the temperature region where the rapid decrease in critical thickness occurred. A small amount of shrinkage of the films also occurred in this region. Finally, shrinkage measurements of unconstrained films indicated that shrinkage was very anisotropic with nearly all of the shrinkage occurring in the plane of the film and very little in the thickness direction.

INTRODUCTION

One limitation of the sol-gel process for forming films is that cracking of the films can occur during drying or heating. For a given sol, a critical film thickness exists above which cracking occurs. The critical thickness is generally <1μm. To produce thicker films, multiple coatings, with a thermal treatment done between each coating, have been used. Besides being time consuming, the multiple coating process produces films that can be heterogeneous in structure since, each layer has experienced a different thermal history.

The existence of a critical cracking thickness for films on substrates has been noted for a variety of materials [1,2] and has also been modeled [3-5]. For films that adhere well to the substrate, the critical thickness, h, is given by:

$$h = (K_{IC}/\sigma\Omega_c(\Sigma))^2 \qquad (1)$$

where K_{IC} is the critical stress intensity factor for the film, σ is the tensile stress in the film, and $\Omega_c(\Sigma)$ is a dimensionless quantity that is a function of the ratio of the Young's modulus of the film to that of the substrate, i.e. $\Sigma = E_f/E_s$. For sol-gel films, several processes occur during processing that generate tensile stresses in the film which can cause cracking.

To form a film by the sol-gel process, a sol film is first formed on the substrate by spin or dip coating. Evaporation of the solvent in the sol takes place during and after coating, which brings the reactive species in

---

the sol closer together, promoting condensation reactions. Usually, the sol will gel before all the solvent has evaporated producing a gel film whose pores are filled with solvent. The removal of the solvent from the pores produces capillary stresses as the solvent meniscus enters the gel.

Several processes occur as the gel film is heated [6-8] which also produce stresses that may lead to cracking. Organic species remaining in the gel after drying are pyrolized. Condensation reactions occur which change the gel structure and can produce shrinkage. Structural relaxation and viscous sintering cause shrinkage at higher temperature. These processes generally occur concurrently at least in some temperature range as the gel is heated.

The goal of this work was to study the cracking behavior of silica sol-gel films prepared under acidic conditions. The effects of the hydrolysis ratio, R (the molar ratio of water to alkoxide in the sol), and temperature on the critical thickness for cracking were determined.

EXPERIMENTAL

Two stock sol solutions, one with ethanol as the solvent and the other with t-butanol, were prepared. The concentrations of components in the stock solutions were 2.15 M tetraethoxysilane (TEOS, manufacturer), 2.15 M deionized water (R=1), and 1.6×10^{-3} M HCl. The TEOS was distilled under partial vacuum prior to use. The stock sols were heated for 27 hr at 55°C and then diluted 2 to 1 with solvent. Three sols were prepared from the ethanol stock sol by adding enough water to obtain R values of 2, 4, and 8 and then heating at 55°C for 16 more hours. The t-butanol stock sol (R=1) was used without any further modification.

The morphology of cracks formed during room temperature drying of films made from the R=4 and R=8 sols was examined using an optical microscope. These films were prepared by spreading a volume of the sol on a glass slide or a silicon wafer, so that the film thickness when dry would be above the critical cracking thickness. Crack growth in these films was observed and video taped using an optical microscope.

The critical cracking thickness of films prepared from the three ethanol based sols and the t-butanol sol was determined as a function of temperature between room temperature and 350°C. Films were cast on glass slides by spreading an appropriate volume of the sol on the slide such that cracking would occur. Films were heated on a hot plate sequentially for 20 min at each soak temperature and the thickness of the thickest uncracked region of a partly cracked film was measured using a profilometer (Dektac).

Thermogravimetric analysis (Dupont) and differential thermal analysis were performed on films made from the R=4 and the R=1 sols that were removed from the substrate after heating to either 80°C (R=4) or 160°C (R=1). The analyses were done in flowing air (50 cc/min) with a heating rate of 5°C/min.

The surface area, pore size distribution and pore volume of films made from these same two sols were determined using nitrogen adsorption analysis. Cracked films were removed from the substrate and analyzed after heating to 160°C.

The shrinkage of constrained (attached to the substrate) and unconstrained (removed from the substrate) films prepared from the R=1 and the R=4 sols was also measured. The films used for constrained shrinkage measurements were spun cast (Headway) at ~2000 rpm and heated to 160°C for 30 min prior to the first thickness measurement. The films were initially ~400 nm thick. Thickness of the constrained films were measured using the profilometer. A portion of the film was etched away with dilute HF or a KOH-isopropanol solution to create a step. Markers were scribed into each

film so that exactly the same location was profiled each time. All films, both constrained and unconstrained, were measured after each 30 min soak in a sequential heating schedule where the films were placed directly in the hot furnace and removed and cooled immediately at the end of the soak.

Several small pieces of film were removed from cracked films made from each sol and photographed using an optical microscope. The same pieces were again photographed at the same magnification after each thermal treatment. The areal shrinkage of each piece was then determined from the micrographs. The thickness of the unconstrained pieces was measured using the profilometer. Care was taken so that only unwarped pieces were measured and that the same location on each piece was profiled after each thermal treatment.

RESULTS AND DISCUSSION

A variety of unusual crack patterns were observed in room temperature dried films prepared from R=4 and R=8 sols. Generally, a network of nearly straight cracks would form first and then curved cracks would nucleate from the straight cracks and grow into the uncracked regions. This result was in agreement with the model of Meakin [9,10,], although, as discussed below, some of the curved cracks had regular forms not predicted by the model. The rate at which cracks grew varied from microns to millimeters per second, indicating stable crack growth. As the film thickness increased beyond the critical thickness, the pieces formed displayed interference fringes indicating that the pieces were warped up from the substrate. For even thicker films, the pieces warped so severely that they became completely detached from the substrate.

Optical micrographs of some of these features are shown in Figure 1. Figure 1a shows cracks in a sinusoidal or sawtooth wave pattern. Sine wave buckles have been seen in films with compressive stress [1,11,12], but this is the first report of sine wave cracks. Another unusual feature present in some of the cracked films were pairs of parallel cracks. These varied in length from tens to hundreds of microns and were generally somewhat curved (see Figure 1b). The two cracks comprising the crack pair nucleated at the

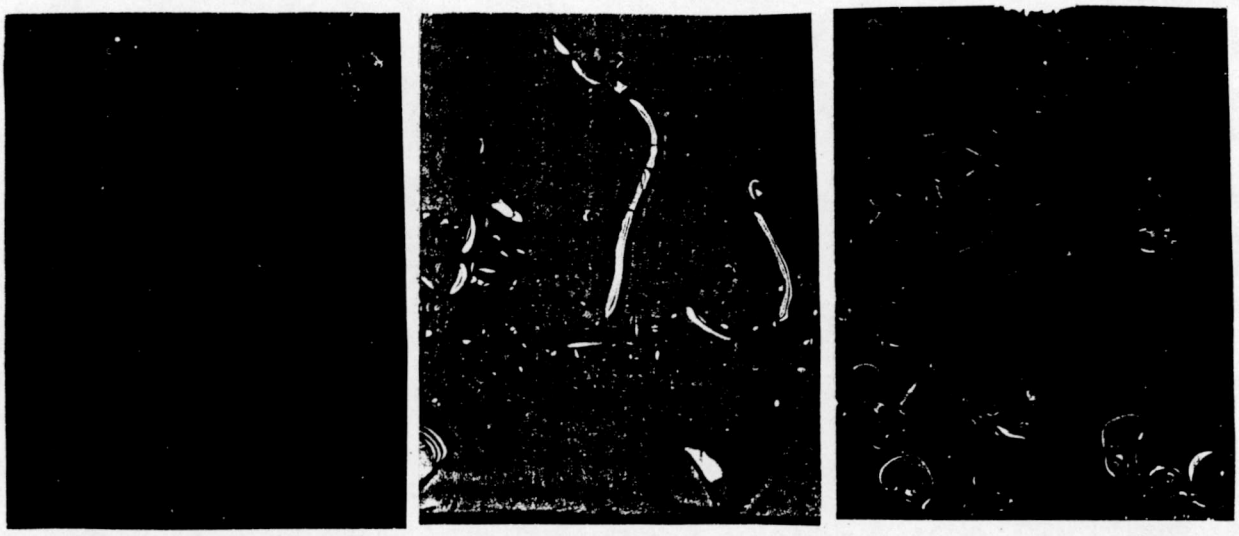

a. b. c.

Figure 1. Crack morphologies produced during drying of sol-gel silica films: a) sinusoidal cracks; b) parallel crack pairs; and c) loop terminated crack pairs.

same time from a preexisting crack and grew at the same rate with a constant separation. Often, other curved cracks would nucleate from the parallel crack pair as it grew and would then grow into the surrounding uncracked areas. Usually, the crack pair would grow until it ran into another preexisting crack. However, sometimes each crack in the pair would curve to the outside and form a loop (see Figure 1c). These unusual crack morphologies must form due to a non-unifrom stress distribution, the causes of which are under investigation.

As mentioned above, the films from the R=4 and R=8 sols gelled after several minutes at room temperature. On the other hand, the films from the R=2 and R=1 sols became tacky liquids at room temperature which gelled when heated to ~140°C. The increase in gelation kinetics with increasing water content is consistent with the increase in condensation rate with extent of hydrolysis [13]. However, nitrogen adsorption analysis on films heated to 160°C indicated that the pore characteristics (pore size distribution, pore volume and surface area) did not vary significantly with R. This may be due to the fact that the pH of the sols was near the isoelectric point of silica where the condensation rate is low [13].

Figure 2 shows that the critical cracking thickness decreased strongly with both increasing water content in the sol and with increasing temperature. There are several possible reasons why the critical cracking thickness decreased with increasing sol water content, even though the pore characteristics of the films did not change. One explanation is that the composition of the liquid in the pores of the gels changes with R. This affects the capillary stress during drying since the stress is proportional to the liquid's surface tension. The higher R is, the richer the pore liquid will be in water, and thus the larger its surface tension will be. Also, for the low R sols, gelation did not occur until well above the boiling points of water and ethanol or t-butanol, so that a solvent phase was not present to produce capillary forces after gelation. This is similar to the results of Schlichting [14], who prepared 10 μm thick, crack-free films which had low water contents since they were hydrolized by exposure to air.

To determine the cause of the decrease in critical cracking thickness with temperature, thermal analysis and shrinkage measurements were performed. The thermogravimetric analysis results (Figure 3) indicated that the low R gel lost weight less gradually and at higher temperature, in the

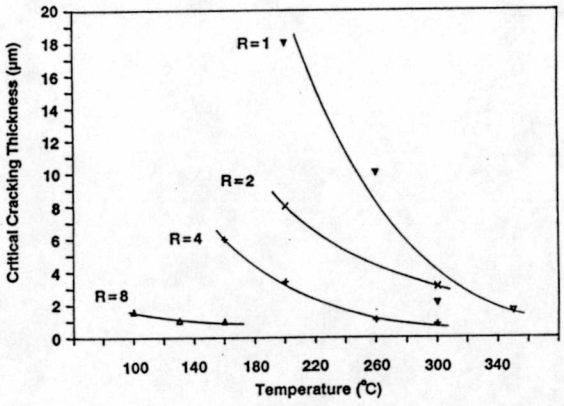

Figure 2

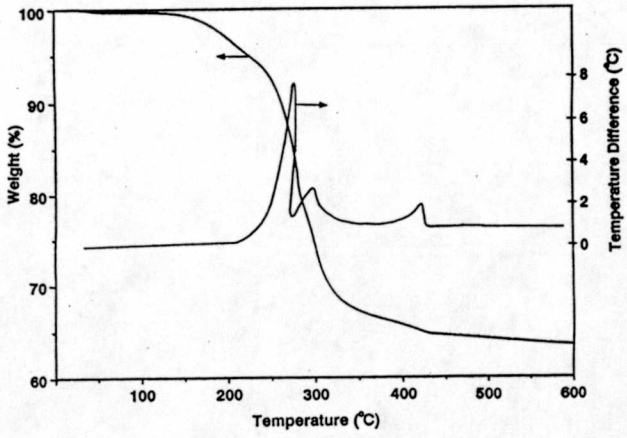

Figure 3

Figure 2. The effect of hydrolysis ratio, R, and temperature on the critical cracking thickness of silica sol-gel films.

Figure 3. Thermogravimetric and differential thermal analyses of the R=1 silica gel, previously heated to 160°C.

range where the critical thickness is sharply decreasing. The differential thermal analysis (Figure 3) indicated that the weight loss of this gel was associated with exothermic reactions. Therefore, the cracking could be due to the disruption of the structure that takes place when the rapid weight loss occurs. Alternately, capillary forces produced when a high boiling point liquid in the pores decomposes could cause cracking. This liquid could consist of siloxane oligimers not bound to the gel structure.

On the other hand, as Figure 4 shows, shrinkage is also occurring in the temperature range where the critical thickness decreases. The constraint of the substrate keeps the film from shrinking in the plane and therfore produces a tensile stress in the film [15]. This stress would be most likely to cause cracking when only a small amount of shrinkage has occurred since the magnitude of the free shrinkage rate, and thus the stress, is high and the structure is porous, and thus weak, at this point [15].

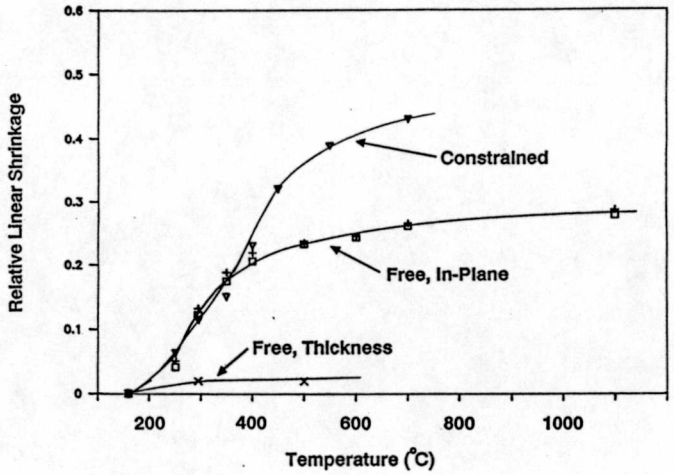

Figure 4. Relative linear shrinkage of unconstrained films prepared from R=4 (x, +) and R=1 (□) sols both in the thickness direction and in the plane, and of a constrained film prepared from the R=1 sol (▽).

As Figure 4 shows, films made from sols with different R values exhibited nearly identical shrinkage behavior as expected from the similar pore characteristics. Unconstrained films shrank in an extremely anisotropic manner, with almost all of the shrinkage occurring in the planar direction. This indicates that structural anisotropy must form in the gel films during constrained drying.

The shrinkage of the constrained film can be compared to that of the unconstrained film using the approach of Scherer [16]. The linear shrinkage rate in the i-direction during constrained sintering of a porous viscous material, $\dot{\varepsilon}_i$, can be written as:

$$\dot{\varepsilon}_i = \dot{\varepsilon}_{i(free)} + (\sigma_i - N(\sigma_j + \sigma_k))/F \qquad (2)$$

where $\dot{\varepsilon}_i(free)$ is the shrinkage rate in the i-direction when the constraint is not present, σ_{i-k} are the stresses in the i, j and k directions caused by the constraint, N is equilivent of the Poisson's ratio which approaches 0.5 as the porosity goes to zero, and F is the resistance to flow which approaches three times the viscosity as the porosity goes to zero. For a constrained film with z as the thickness direction, $\sigma_z=0$, $\dot{\varepsilon}_x=\dot{\varepsilon}_y=0$, $\dot{\varepsilon}_{x(free)} = \dot{\varepsilon}_{y(free)} = \dot{\varepsilon}_{free}$ and, for the present case, as Figure 4 shows, $\dot{\varepsilon}_{z(free)} \approx 0$. Using these substitutions in equation (2) and solving for $\dot{\varepsilon}_z$ gives:

$$\dot{\varepsilon}_z = [2N/(1-N)]\ \dot{\varepsilon}_{free} \qquad (3)$$

Since the value of N is approximately half of the relative density [17], equation 2 predicts that the linear shrinkage rate of the constrained film in the thickness direction should be less than that of the free film in the plane at low densities and greater than it at higher densities. This is consistent with the data in Figure 4.

CONCLUSIONS

Silica films prepared from acidic sols with low values of R do not crack at temperatures below 200°C unless they are thicker than 10 μm. However, their critical cracking thickness rapidly decreases between 250° and 350°C to about 1 μm, a value close to that of films made from high R sols. Film shrinkage and reactions causing weight loss occur in this temperature range. Finally, drying causes the structure of the films to be anisotropic in such a manner as to cause them to shrink primarily in the plane during heating, when free from the constraint of the substrate.

ACKNOWLEDGEMENTS

This work was sponsored by the Department of Energy, Contract DE-AC04.76-DP00789. The author is grateful to M. S. Harrington, D. Goodnow and C. S. Ashley for experimental assistance and to R. W. Schwartz for reviewing the manuscript.

REFERENCES

1. K.L. Chopra, Thin Film Phenomena, (McGraw-Hill Book Co., New York, 1969), pp. 311-313.
2. S.G. Shyu, T.J. Smith, S. Baskaran, and R.C. Buchanan in Better Ceramics Through Chemistry III, edited by C.J. Brinker, D.E. Clark and D.R. Ulrich (Mat. Res. Soc. Proc. 121, Pittsburgh, PA 1988) pp. 767-73.
3. M.S. Hu and A.G. Evans, Acta Metall. 37, 917 (1989).
4. M.S. Hu, M.D. Thouless and A.G. Evans, Acta Metall. 36, 1301 (1988).
5. G. Gille, Thin Solid Films 111, 201 (1984).
6. C.J. Brinker, G.W. Scherer and E.P. Roth, J. Non-Cryst. Sol. 72, 345 (1985).
7. P.F. James, J. Non-Cryst. Solids 100, 93 (1988).
8. F. Orgaz-Orgaz, J. Non-Cryst. Solids 100, 115 (1988).
9. P. Meakin, Thin Solid Films 151, 165 (1987).
10. A.T. Skjeltorp and P. Meakin, Nature 335, 424 (1988).
11. A. Alnaimi and S. Berg, in The Proceedings of the Eighth International Vacuum Congress, edited by F. Abeles and M. Croset, p. 336.
12. C. Weissmantel, C. Schurer, F. Frohlich, P. Grau, and H. Lehmann, Thin Solid Films 61, L5 (1979).
13. C.J. Brinker, J. Non-Cryst. Solids 100, 31 (1988).
14. J. Schlichting, J. Non-Cryst. Solids 63, 173 (1984)
15. G. W. Scherer and T. Garino, J. Am. Ceram. Soc. 68, 216 (1985).
16. G.W. Scherer, J. Non-Cryst. Solids 34, 239 (1979).
17. T.J. Garino and H.K. Bowen, J. Am. Ceram. Soc., 73, 251 (1990).

DISCLAIMER